

The transition to nonlinearity and new constraints on biasing

Roman Juszkiewicz^{1,2,3} & Enrique Gaztañaga^{4,5}

¹ J. Kepler Astronomical Center, 65-265 Zielona Góra, Poland

² Département de Physique Théorique, Université de Genève, CH-1211 Genève, Switzerland

³ N. Copernicus Astronomical Center, 00-716 Warsaw, Poland

⁴ INAOE, Astrofísica, Tonantzintla, Apdo Postal 216 y 51, Puebla 7200, Mexico

⁵ Institut d'Estudis Espacials de Catalunya, IEEC/CSIC, Edf. Nexus-201 - c/ Gran Capitan 2-4, 08034 Barcelona, Spain

Abstract.

We present two new dynamical tests of the biasing hypothesis. The first is based on the amplitude and the shape of the galaxy-galaxy correlation function, $\xi_g(r)$, where r is the separation of the galaxy pair. The second test uses the mean relative peculiar velocity for galaxy pairs, $v_{12}(r)$. This quantity is a measure of the rate of growth of clustering and it is related to the two-point correlation function for the matter density fluctuations, $\xi(r)$. Under the assumption that galaxies trace the mass ($\xi_g = \xi$), the expected relative velocity can be calculated directly from the observed galaxy clustering. The above assumption can be tested by confronting the expected v_{12} with direct measurements from velocity-distance surveys. Both our methods are checked against N-body experiments and then compared with the $\xi_g(r)$ and v_{12} estimated from the APM galaxy survey and the Mark III catalogue, respectively. Our results suggest that cosmological density parameter is low, $\Omega_m \approx 0.3$, and that the APM galaxies trace the mass at separations $r \gtrsim 5 h^{-1}\text{Mpc}$, where h is the Hubble constant in units of $100 \text{ km s}^{-1}\text{Mpc}$. The present results agree with earlier studies, based on comparing higher order correlations in the APM with weakly non-linear perturbation theory. Both approaches constrain the linear bias factor to be within 20% of unity. If the existence of the feature we identified in the APM $\xi_g(r)$ – the inflection point near $\xi_g = 1$ – is confirmed by more accurate surveys, we may have discovered gravity's smoking gun: the long awaited “shoulder” in ξ , generated by gravitational dynamics and predicted by Gott and Rees 25 years ago.

1. Introduction

We have been recently working on two projects, directly related to the topic of this Meeting – the transition to nonlinearity in gravitational clustering. We

have therefore decided to present some of our results here. The first idea – to use the inflection point in the galaxy-galaxy correlation function to constrain biasing is in a more mature state than the second, which uses measurements of the relative motions in pairs of galaxies. Accordingly, the first project is almost a paper – it has been submitted for publication in *Monthly Notices*. The results of our work on the second project are still far from completion but ripe enough to be presented and discussed.

1.1. The CDM crisis and biasing

The concept that galaxies may not be fair tracers of the mass distribution was introduced in the early eighties, in part in response to the observation that galaxies of different morphological types have different spatial distributions, hence they cannot all trace the mass (there are two excellent reviews on the subject: Strauss & Willick 1995 and Hamilton 1998). However, there was also another reason: to “satisfy the theoretical desire for a flat universe” (Davis et al. 1985, p.391). More precisely, biasing was introduced to reconcile the observations with the predictions of the Einstein-de Sitter cold dark matter (CDM) dominated model. At the time, it seemed that just a simple rescaling of the overall clustering amplitude by setting $\xi_g(r) = b^2 \xi(r)$, where $b \approx 2$ might do the job (Davis et al. 1985). However, very soon thereafter, it became clear that this is not enough: while the unbiased ($b = 1$) $\xi(r)$ had too large an amplitude at small r , the biased model did not have enough large-scale power to explain the observed bulk motions (Vittorio et al. 1987). A similar conclusion could be drawn from comparison of the relative amplitude of clustering on large and small scales (eg Maddox et al 1990). The problem with the shape of $\xi(r)$ became explicit when measurements of $\xi_g(r)$ showed that the optically selected galaxies follow an almost perfect power law over nearly three orders of magnitude in separation. This result disagrees with N-body simulations. The standard ($\Omega_m = 1$) CDM model as well as its various modifications, including $\Omega_m < 1$ and a possible non-zero cosmological constant, fail to match the observed power law (see Fig 11-12 in Gaztañaga 1995, Jenkins et al. 1998; most of these problems were already diagnosed by Davis et al. 1985). Two alternative ways out of this impasse were recently discussed by Rees (1999) and Peebles (1999). We believe that it will be helpful to discuss both approaches because their existence provides the motivation for our work.

1.2. Environmental cosmology

A possible response to the CDM crisis is to build a model where simple phenomena, like the power-law behavior of ξ_g are much more complicated than they seem. In particular, one can explore the possibility that the emergence of large scale structure is not driven by gravity alone but by “environmental cosmology” – a complex mixture of gravity, star formation and dissipative hydrodynamics (Rees 1999). A phenomenological formalism, appropriate for this approach was recently proposed Dekel & Lahav (1999). According to the old, “linear biasing” prescription, at each smoothing scale, the galaxy- and the dark matter-density fields, δ_g and δ , are related by the linear function

$$\delta_g = b \delta , \quad (1)$$

where b is a time- and scale-independent constant. In the new picture, the relationship between the two fields is neither linear nor deterministic. The biasing factor, here defined as the ratio of the rms values of the two fields, $b = \sigma_g/\sigma$ is allowed to depend on the smoothing scale as well as on the cosmological time. A convenient measure of the stochasticity in the relationship between the two fields is the cross-correlation coefficient,

$$R \equiv \frac{\langle \delta \delta_g \rangle}{\sigma_g \sigma} ; \quad |R| \leq 1 . \quad (2)$$

The special case $R = 1$ describes the deterministic bias, while $R = 0$ corresponds to the “maximum stochasticity”, or the case when the two fields are completely uncorrelated. The parameters R and b describe the biasing and stochasticity in the galaxy distribution relative to the spatial mass distribution. When referring to specific galaxy surveys, we will sometimes use subscripts, e.g. b_{IRAS} for the *IRAS* survey. These quantities should be distinguished from the bias and stochasticity measures for two classes of galaxies of different morphological types, e.g. for early (subscript e) and late (subscript l) galaxies: $b_{el} \equiv \sigma_e/\sigma_l$, and $R_{el} \equiv \langle \delta_e \delta_l \rangle (\sigma_e \sigma_l)^{-1}$.

The above parameters can be estimated or constrained by more or less direct measurements from galaxy redshift surveys, peculiar velocity data and other observations. They can be also studied in semi-analytic theoretical models (Seljak 2000, Scoccimarro et al. 2000), hydrodynamic simulations or semi-analytic models combined with N-body simulations (eg. Blanton et al. 2000, Somerville et al. 2001 and references therein).

1.3. Constraints on biasing

If biasing is indeed important and complicated, we should expect that b, b_{el}, R and R_{el} are all significantly different from unity and scale-dependent. As we show below, at sufficiently large scales, $r \gtrsim 10h^{-1}\text{Mpc}$, there is actually evidence to the contrary: the admissible deviations of b and R are small and always comparable to the accuracy of the measurements.

Skewness and higher moments. The strongest constraints on large (weakly non-linear) scales come from the measurements of the two-, three- and four-point connected moments of the density field in the APM catalogue. These constraints are obtained as follows. One assumes that galaxies trace the mass and the large-scale structure we observe today grew out of small-amplitude, Gaussian density fluctuations in an expanding, self-gravitating non-relativistic gas. If our assumption is correct, by now nonlinear gravitational instability would have driven the distribution away from gaussianity, generating skewness and higher connected moments, which can be calculated analytically (Juszkiewicz et al. 1993, Bernardeau 1994a, 1994b). The assumptions about initial gaussianity and lack of biasing can then be tested by comparing the analytical predictions with observations. The predictions are in good agreement with the data from the APM (Gaztañaga 1994, Gaztañaga & Frieman 1994, Frieman & Gaztañaga 1999) as well as the IRAS PSCz catalogue (Feldman et al. 2000) and suggest that $b(r)$ is within 20% of unity for $r \gtrsim 10h^{-1}\text{Mpc}$, or at linear scales (where the clustering amplitude is less than unity).

Redshift distortions. Some of the most radical claims that b_{el} can be as large as 1.5 to 2 are based on comparisons of the estimates of the strength of clustering in the 1.2 Jy IRAS catalogue with optical redshift surveys (Strauss & Willick 1995 and references therein). Indeed, those earlier studies, summarized by Hamilton (1998), gave a redshift distortion parameter $\beta_{IRAS} = \Omega_m^{0.6}/b_{IRAS} = 0.77 \pm 0.22$, while the average and the standard deviation of the same parameter, obtained from optical surveys is, according to the same compilation, $\beta_{optical} = 0.52 \pm 0.26$, implying a relative bias $b_{optical}/b_{IRAS} = b_{el} \approx 1.5$. The most recent analysis (Hamilton et al. 2000) of the larger PSCz sample Saunders et al. 2000 gives $\beta_{IRAS} = 0.41 \pm 0.13$, consistent with $b_{el} = 1$. Moreover, Hamilton et al. also conclude that their results are consistent with $R_{IRAS}(r) \approx 1$ at $r \gtrsim 10h^{-1}\text{Mpc}$. More recently Hamilton and Tegmark (2000) have studied the large as well as small-scale clustering in real space, reconstructed from the redshift space data of the PSCz survey and found evidence for scale-dependent bias; however, the effect is significant at small, strongly-nonlinear scales only.

Large scale flows. Recent measurements of the mean relative pairwise velocity of galaxies allow an independent estimate of Ω_m and the biasing parameter. These results are consistent with $\Omega_m \approx 0.3$ and $R \approx b \approx 1$, $b_{el} \approx R_{el} \approx 1$ at separations $r \gtrsim 5h^{-1}\text{Mpc}$ (Juszkiewicz et al. 2000a).

Weak lensing. The values of b and Ω_m , derived from large scale flows are consistent with recent measurements of cosmic shear correlations based on the VIRMOS deep imaging survey (Van Waerbeke et al. 2001). On much smaller scales, $r \approx 1h^{-1}\text{Mpc}$, weak lensing data from the Sloan Survey give $\Omega_m R/b \approx 0.3$ (Fischer et al. 1999), again in agreement with the estimates from the pairwise motions, although unlike the relative velocity approach, the Sloan results suffer from degeneracies between Ω_m and bias.

Qualitative arguments. Qualitatively, strong biasing effects would be difficult to reconcile with the well known fact that the L_* galaxies, dwarf galaxies and IRAS galaxies have strikingly similar distributions, all avoiding the voids (Peebles 1993, pp. 638-642). Another empirical argument against biasing is provided by the universal character of the observed Tully-Fisher and fundamental plane relations (see, for example Binney 1999; Peebles 1999).

Simulations. All simulations of the galaxy formation process, either of hydrodynamic or semi-analytic variety predict morphological segregation as well as b and R parameters dependent on scale and time. Since these models are at a relatively early stage of their development, the details differ from model to model on small scales and at high redshifts, i.e. exactly where their b and R parameters are significantly different from unity and where clustering is strongly nonlinear. However, most of these numerical experiments broadly agree that with decreasing redshift and increasing scales, b and R approach unity (see e.g. Figure 18 in Somerville et al. 2001 and references therein).

In the end, it may turn out that to explain the observed structure, all we need is just the plain gravitational instability theory, leaving complex non-gravitational physics on scales below a Megaparsec to cosmogony, directly involving star formation. We discuss this possibility below.

1.4. What you get is what you see

An obvious alternative to environmental cosmology was recently discussed by Peebles (1999), who pointed out that “as Kuhn has taught us, complex interpretations of simple phenomena have been known to be precursors of paradigm shifts” and perhaps after fifteen years of attempts to salvage the CDM model with biasing, it is time to abandon this approach, as well as the biasing hypothesis itself as “another phlogiston” (all quotations in inverted commas are from Peebles 1999). Instead, one can explore a simpler option, that galaxies trace the mass distribution, or

$$\xi_g = \xi \text{ and } R = b = 1, \quad (3)$$

at least for local (low redshift), optically selected galaxies with a broad magnitude sampling. This approach rests on the idea that no matter how or where galaxies form, they must eventually fall into the dominant gravitational wells and therefore trace the underlying mass distribution (see Peebles 1980, hereafter LSS; Fry 1996). Our purpose here is to test this idea, using measurements of relative velocities of pairs of galaxies and the shape of the two-point correlation function.

1.5. Outline of the paper

In this paper we propose two new tests of the biasing hypothesis, which involve two measures of clustering. The first is the two-point correlation function of mass density fluctuations, ξ . The second is a measure of the rate of gravitational clustering – the relative velocity of particle pairs, v_{12} . We describe our theoretical model in the next section. Our analytic formulae used to test the biasing hypothesis are checked against N-body simulations in §3. In §4 we apply our tests to the APM galaxy survey. Finally, in §5 we summarize and discuss our results.

2. Theory

2.1. The relative velocity

The relative pairwise velocity v_{12} was introduced in the context of the BBGKY theory (Davis and Peebles 1977), describing the dynamical evolution of a collection of particles interacting through gravity. In this discrete picture, \vec{v}_{12} is defined as the mean value of the peculiar velocity difference of a particle pair at separation \vec{r} (LSS, Eq. 71.4). In the fluid limit, its analogue is the pair-density weighted relative velocity Fisher et al. 1994, Juszkiewicz et al. 1998,

$$\vec{v}_{12}(r) = \frac{\langle (\vec{v}_1 - \vec{v}_2)(1 + \delta_1)(1 + \delta_2) \rangle}{1 + \xi(r)}, \quad (4)$$

where \vec{v}_A and $\delta_A = \rho_A/\langle \rho \rangle - 1$ are the peculiar velocity and fractional density contrast of matter at a point $A = 1, 2, \dots$. The brackets $\langle \dots \rangle$ denote ensemble averages for pairs of points at a fixed separation $r = |\vec{r}_1 - \vec{r}_2|$, while $\xi(r) = \langle \delta_1 \delta_2 \rangle$. In gravitational instability theory, the magnitude of $\vec{v}_{12}(r)$ is related to $\xi(r)$ through the pair conservation equation (LSS, Eq. 71.6).

Recently Juszkiewicz et al. (1999, hereafter JSD) have proposed an approximate solution of the pair conservation equation. Using Eulerian perturbation theory, they solved the equation for $v_{12}(r)$ to second order in ξ . They also proposed an interpolation between their large- r perturbative limit, and the well known small separation limit – the stable clustering solution, $v_{12}(r) = -Hr$, where H is the Hubble constant (LSS, §71). The resulting ansatz is given by

$$v_{12}(r) = -\frac{2}{3} H f r \bar{\xi}(r) [1 + \alpha \bar{\xi}(r)] , \quad (5)$$

$$\bar{\xi}(r) = (3/r^3) \int_0^r \xi(x) x^2 dx \equiv \bar{\xi}(r) [1 + \xi(r)] . \quad (6)$$

Here α is a parameter, determined by the logarithmic slope of $\xi(r)$, while $f = d \ln D / d \ln a$, with $D(a)$ being the standard linear growing mode solution and a – the cosmological expansion factor (LSS, §11). The solution (5) assumes Gaussian initial conditions, and the dynamics of clustering is assumed to be dominated by the gravity of inhomogeneities in a pressure-less fluid of non-relativistic particles. For all such models, including those with a non-zero cosmological constant, $f \approx \Omega_m^{0.6}$ (Peebles 1993, §13). If the correlation function is given by a pure power law, $\xi \propto r^{-\gamma}$, where $0 < \gamma < 3$, the parameter α is given by

$$\alpha \approx 1.2 - 0.65 \gamma . \quad (7)$$

This formalism can be generalized for a non-power law $\xi(r)$ by replacing γ in Eq. (7) with an effective slope,

$$\gamma_o \equiv -d \ln \xi / d \ln r |_{r_o} , \quad (8)$$

evaluated at separation $r = r_o$, defined by the condition

$$\xi(r_o) = 1 . \quad (9)$$

JSD tested the equations (5) - (9) against high resolution N-body simulations, provided by the Virgo consortium (Jenkins et al. 1998). They found an excellent agreement between the streaming velocity, predicted by their ansatz and the $v_{12}(r)$, measured from the simulations in the entire dynamical range, $0.1 < \xi < 10^3$. However, the N-body experiments they used were confined to four different CDM-like models, considered by Jenkins et al. (1998). As we have already pointed out in the Introduction, models of this kind fail to reproduce the observed $\xi_g(r)$ unless one resorts to a highly contrived, scale- and time-dependent biasing function (Gaztañaga 1995, Jenkins et al. 1998, Peebles 1999). One of our objectives here is to test the validity JSD ansatz for $v_{12}(r)$ against a new set of N-body simulations, which differ significantly from those originally considered by JSD. Here we use simulations with a more realistic $\xi(r)$, inferred by Baugh & Gaztañaga (1996) from the measurements of galaxy-galaxy correlations in the APM survey (see the description below; from now on, we will refer to these numerical experiments and their initial conditions as APM-like).

2.2. The inflection point

In the gravitational instability theory, newly forming mass clumps are generally expected to collapse before relaxing to virial equilibrium. If this were so, $|v_{12}(r)|$

would have to be larger than the Hubble velocity Hr to make $v_{12}(r) + Hr$ negative. As a consequence, the slope of ξ ,

$$d \ln \xi(r) / d \ln r = -\gamma(r), \quad (10)$$

must increase at separations where $\xi(r, t) \approx 1$. This effect was recognized long ago by Gott & Rees (1975). When the expected “shoulder” was not found in the observed galaxy-galaxy correlation function, Davis & Peebles (1976) introduced the so-called pre-virialization conjecture as a way of reducing the size of the jump in $\gamma(r)$ (the conjecture involves non-radial motions within the collapsing clump; see the discussion in LSS, §71 and Peebles 1993, pp. 535 - 541; see also Villumsen & Davis 1986; Łokas et al. 1996 and Scoccimarro & Frieman 1996). Later observational work showed a clear break in the shape of ξ for several redshift and angular catalogues, which was early evidence for the linear to non-linear transition, pointed out by Guzzo and collaborators (see the review by Guzzo 1997).

The arguments, raised by Peebles and Davis (1976) were qualitative rather than quantitative. Quarter a century later the precision of N-body simulations as well as the quality of the observational data have improved dramatically enough to justify a reexamination of the problem. The actual shape of the correlation function near $\xi = 1$ can be investigated with high resolution N-body simulations like those run by the Virgo Consortium (Jenkins et al. 1998). In all four of the Virgo models, the slope of $\xi(r)$ exhibits a striking feature. Instead of a shoulder, or a simple discontinuity in $\gamma(r)$, however, $\xi(r)$ has an inflection point,

$$d^2 \xi(r) / dr^2 = 0, \quad (11)$$

which occurs at a uniquely defined separation $r = r_*$. At this separation, the logarithmic slope of ξ reaches a local maximum, $d \ln \xi / d \ln r = -\gamma_*$. In all four of the models JSD investigated, the inflection point indeed appears near the transition $\xi = 1$, as expected by the earlier speculations, involving the “shoulder” in ξ . Namely, r_* is almost identical with the scale of nonlinearity:

$$r_* \approx r_o. \quad (12)$$

More precisely, a comparison of Figure 1 in JSD with Figure 8 in Jenkins et al. (1998) gives

$$|r_o - r_*| < 0.1 r_o \quad (13)$$

for all four considered models. Moreover, for all models, studied by JSD, the $-\gamma$ vs. r dependence can be described as an S-shaped curve, with a maximum at $r = r_* \approx r_o$, and a minimum at a smaller separation. For $r \geq r_*$, the nonlinear slope (measured from Virgo simulations) follows the linear $\gamma(r)$, determined by the initial conditions. The separation r_* is therefore also the branching point between the linear and nonlinear $\gamma(r)$ curves, which are identical for $r > r_*$ (actually, they differ a little; the small differences between the two curves can be entirely attributed to sampling errors in the N-body experiments; see Figure 1 in JSD). This property can be used to identify r_* in noisy simulations, and/or observations, when the noise in the measured $\gamma(r)$ curve does not allow a direct determination of r_* as the position of the maximum in $-\gamma(r)$.

If the relation (12) is indeed a general property of gravitational clustering, it can be used as a test of biasing as follows. Suppose the biasing factor is a scale-independent constant, significantly greater than unity: $b \gg 1$. Then $\xi_g \gg \xi$ and the relation (12) will break down. For a power-law correlation function, $\xi_g(r) = (r_o/r)^\gamma = b^2 \xi(r)$, and instead of equation (12) we will have

$$r_* \approx r_o b^{-2/\gamma}. \quad (14)$$

Since the observed slope is $\gamma \approx 1.8$, for $b = 2$, the shoulder in the correlation function should appear at a separation smaller than a half of the r_o ! The above argument can be generalized to a broader class of models, allowing scale-dependent bias provided $b(r)$ is a smooth monotonic function and $b(r_o)$ is significantly greater than unity. Whenever these conditions apply, strong biasing always implies $r_o \gg r_*$. Hence, the comparison of these two scales determined from observations can be used as a diagnostic for biasing.

3. N-body simulations

3.1. Initial conditions

In this section, we compare our ansatz for $v_{12}(r)$ with the results from P³M simulations. We use APM-like models for the initial shape of $P(k)$ in Baugh & Gaztañaga (1996). The box size is $600 h^{-1}$ Mpc (or $300 h^{-1}$ Mpc) with 200^3 (or 100^3) dark matter particles. The APM-like models have Gaussian initial conditions with a power spectrum inferred from correlations in the APM survey, following the procedure, introduced by Baugh & Gaztañaga 1996. The power spectrum of the density fluctuations is related to $\xi(r)$ through the usual Fourier transform,

$$P(k) = \int \xi(r) \exp(i\mathbf{k} \cdot \mathbf{r}) d^3r. \quad (15)$$

Following the prescription of Baugh & Gaztañaga, we assume an initial power spectrum of the form

$$P(k) = \frac{Ak}{\left(1 + (k/0.05h \text{ Mpc}^{-1})^2\right)^{1.6}}. \quad (16)$$

The linear spectrum, given above is designed to evolve into a nonlinear one, matching the APM measurements of $P(k)$ under the assumption of no bias. The normalization constant A is directly related to the degree of inhomogeneity of the mass distribution at the end of the simulation, parametrized by σ_8 – the rms mass density contrast, measured in spheres of a radius of $8 h^{-1}$ Mpc. Following Baugh and Gaztañaga, we choose the constant A in order to ensure that at the end of the simulation, $\sigma_8 = 0.85$. The quality of the agreement of the evolved $\xi(r)$ with the APM data at small separations, where $\xi \gg 1$, depends on the assumed value of Ω_m . However, as we show below, for $r \geq 2h^{-1}$ Mpc and $\xi < 3$, this effect is negligible (compare Figures 1 and 3). This range of separations and clustering amplitudes brackets from both sides the region, on which we focus on here: the transition between $\xi < 1$ and $\xi > 1$. We use simulations with $\Lambda = 0$ and two different values of the density parameter: $\Omega_m = 1$ and 0.3 .

3.2. Estimators

Two different estimators for $\xi(r)$ and v_{12} are used. To construct the first estimator, we cut the simulation box into cubical pixels of size Δ_l , placed on a regular lattice. The density fluctuation amplitude at the i th pixel is

$$\delta_i = \frac{N_i}{\langle N \rangle} - 1, \quad (17)$$

where N_i is the particle count in that pixel. The estimator for the two-point function is then:

$$\hat{\xi}^{(1)}(r) = \frac{1}{N_r} \sum_{i,j} \delta_i \delta_j W_{ij}(r), \quad (18)$$

where

$$N_r = \sum_{i,j} W_{ij}(r) \quad (19)$$

is the number of pairs of pixels at separation r in the sampled region, and the window function $W_{ij}(r) = 1$ if pixels i and j are separated by $|\vec{r}_i - \vec{r}_j| = r \pm \Delta r$, and 0 otherwise. For the pairwise velocity we define as \hat{v}_i the average velocity in the i th pixel at position \vec{r}_i . We can then use an equivalent expression for the first estimator of v_{12} :

$$\hat{v}^{(1)}(r) = \sum_{i,j} (\vec{v}_i - \vec{v}_j) \cdot \hat{r}_{ij} U_{ij}(r), \quad (20)$$

where

$$\hat{r}_{ij} \equiv \frac{\vec{r}_i - \vec{r}_j}{|\vec{r}_i - \vec{r}_j|} \quad (21)$$

is a unit vector separating pixels i and j and the sum is over all pairs of pixels, while

$$U_{ij} \equiv \frac{(1 + \delta_i) (1 + \delta_j) W_{ij}(r)}{N_r [1 + \xi(r)]}. \quad (22)$$

The second estimator uses all of the particle pairs rather than the counts in pixel pairs:

$$\hat{\xi}^{(2)}(r) = \frac{1}{\langle n \rangle V_r} \sum_{i>j} W'_{ij}(r) - 1, \quad (23)$$

where now the window function $W'_{ij}(r) = 1$ if particles i and j are separated by $|\vec{r}_i - \vec{r}_j| = r \pm \Delta r$, $\langle n \rangle$ is the mean particle density and V_r is the volume of the spherical shell of radius r and thickness Δr . Typically, $\langle n \rangle V_r$ is estimated from a random catalogue of particles, drawn from the same sample, because the effective volume, containing the pairs separated by a distance $r \pm \Delta r$ might depend on the geometry. However, our simulations use a large and periodic box, with no boundaries and high densities (not affected by shot-noise at the scales of interest). So the above expression gives a good and quick estimator. The corresponding estimator for the pairwise velocity is

$$\hat{v}^{(2)}(r) = \frac{\sum_{i>j} (\vec{v}_i - \vec{v}_j) \cdot \hat{r}_{ij} W'_{ij}(r)}{\sum_{i>j} W'_{ij}(r)} \quad (24)$$

where v_i and v_j are now individual particle velocities. Note that this estimator does not depend on the effective volume of the shell, V_r .

Both estimators agree reasonably well in our simulations. The first set is more useful (faster to run) for large separations, as we can reduce the resolution of the lattice and have a relatively small number of pixels. The second set is more adequate (faster to run) for the small separations.

3.3. The correlation function

The evolved, nonlinear correlation functions, measured from simulations are shown in Figure 1 (top panel). The full squares correspond to the $\Omega_m = 1$ model, while the open squares represent $\Omega_m = 0.3$. For comparison, we show the linear correlation function (dashed line), scaled from some “initial” redshift z_o to the present ($z = 0$), following the linear theory expression for the Einstein-de Sitter model, $\xi(r, 0) = \xi(r, z_o)(1+z_o)^2$. Nonlinear effects are more pronounced in the low density model. This happens because of the well known suppression of linear growth, which occurs at late times ($z < 1/\Omega_m$) in low density models and leads to the enhanced clustering on small scales relative to large scales.

Note however, that although the correlation functions differ significantly in amplitude at separations $r < 2h^{-1}\text{Mpc}$, their slopes $\gamma(r)$ are almost indistinguishable (Figure 1, bottom panel).

The particle resolution (the Nyquist wavelength $\propto N^{-1/3}$) of the simulations used here is significantly lower than the resolution of Virgo simulations, and the noise in the measured $\xi(r)$ is further amplified by differentiating over r . As a result, determining the position of the inflection point r_* directly from the $\gamma(r)$ curve alone is difficult. To overcome this problem, we identify r_* by comparing the linear and nonlinear $\gamma(r)$ curves. Taking r_* to be the separation at which the nonlinear slope drops below the linear slope in Figure 3, as described earlier, we get

$$r_* \simeq 5 h^{-1}\text{Mpc} \approx r_o, \quad (25)$$

in excellent agreement with equation (13). Hence, the equality between r_* and r_o can probably be considered as a generic outcome of gravitational dynamical evolution in a model where galaxies trace the mass and the initial slope, $d \ln \xi / d \ln r$, is a smooth decreasing function of the separation r . Such a picture is also known as hierarchical clustering; an obvious additional condition to make sure that small scale clumps collapse before the large scale ones, is $\gamma > 0$, see e.g. LSS.

3.4. The relative velocity

In this section we describe N-body tests of the JSD model for the relative motions in pairs of galaxies. We consider two models with APM-like initial spectra: an Einstein-de Sitter model and an open model with $\Omega_m = 0.3$. For both models, the theoretical predictions for the mean pairwise velocity, based on equation (5), are plotted in Figure 2 as continuous lines. These predictions can be compared with N-body measurements, shown as full squares for the $\Omega_m = 1$ model and as open squares for $\Omega_m = 0.3$. The agreement between the theoretical and experimental $v_{12}(r)$ curves shows that our ansatz provides a good approximation of the N-body results in the entire dynamical range probed

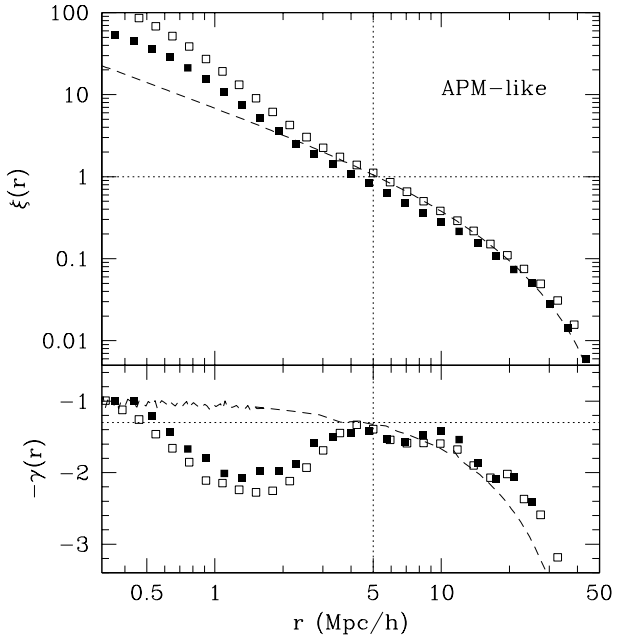


Figure 1. The top panel shows the linear correlation function (dashed line) and the measured non-linear $\xi(r)$, obtained from the APM-like simulations with density parameters $\Omega_m = 0.3$ (open squares) and $\Omega_m = 1.0$ (full squares). The bottom panel shows the corresponding logarithmic slope, $-\gamma(r) = d \ln \xi / d \ln r$ for each of the three curves from the top panel. The vertical dotted line shows the separation r_o , defined by the condition $\xi(r_o) = 1$ (top) and the separation r_* , at which the non-linear $\gamma(r)$ curve crosses the linear one (bottom).

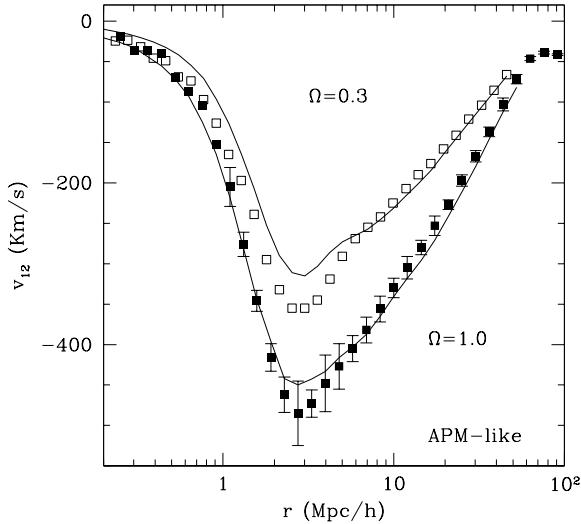


Figure 2. The mean pairwise velocity $v_{12}(r)$, measured from two sets of APM-like simulations with $\Omega_m = 0.3$ (open squares) and $\Omega_m = 1.0$ (full squares), are compared with an approximate analytical solution of the pair conservation equation (eq. [5]; continuous lines).

for both models. The mean and errors in the $\Omega_m = 1$ simulations come from the mean and dispersion, obtained from five independent realizations of the APM-like model. For the open model ($\Omega_m = 0.3$, open squares) we used only one realization, but the expected sampling variance is expected to be the same. Indeed, the initial $P(k)$ is identical in both cases. Moreover, the long-wave tails of the *final* power spectra (which determine the size of the sampling error bars) are also identical because they are not affected by the nonlinear evolution.

4. Comparison with observations

4.1. The correlation function

The measurements of $\xi_g(r)$, and $\gamma(r) \equiv -d \ln \xi_g / d \ln r$, obtained from the angular correlations of galaxy pairs in the APM catalogue (Baugh 1996), are plotted in Figure 3. The top panel shows the two-point function (points with error bars), and the linear theory curve, described in §3.3 (dashed line). The intersection of the two perpendicular dotted lines marks the point $(\xi_g, r) = (1, r_o)$. The bottom panel of Figure 3 shows the APM $\gamma(r)$ as a function of the pair separation r . Note the remarkable similarity between the empirical data and the characteristic peak in the $\gamma(r)$ found in the simulations (Figure 1). The intersection of the two mutually perpendicular, dotted lines in the bottom panel of Figure 3 marks the crossing between the linear model for $\gamma(r)$ (dashed line) and the nonlinear $\gamma(r)$ curve, determined from the APM catalogue. The crossing occurs at the

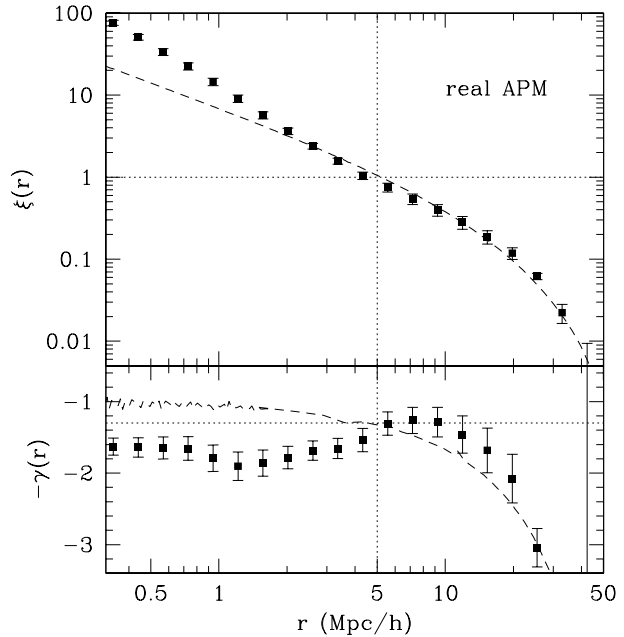


Figure 3. The spatial correlation function of APM galaxies (top panel, symbols with errorbars), compared to the linear theory APM-like model, described earlier (top panel, dashed line). The bottom panel shows the corresponding logarithmic slope, $\gamma(r)$. The intersection of the two perpendicular dotted lines marks the points where $\xi \simeq 1$ (top) and where the non-linear slope crosses the linear one (bottom).

separation $r \simeq 5 h^{-1}\text{Mpc}$, and to first approximation this scale could be identified with r_* . However, a closer inspection of our Figure 3 suggests that, given the error bars, the actual position the peak could be shifted to the right, to a somewhat larger separation. Taking into account the error bars in Figure 3 as well as the uncertainties in the assumed linear theory slope, we obtain

$$r_* \simeq (6 \pm 1) h^{-1}\text{Mpc} , \quad (26)$$

and

$$r_o \simeq (5 \pm 1) h^{-1}\text{Mpc} . \quad (27)$$

The slope at $r = r_*$ is $\gamma_* \simeq -1.4$. If we assume the linear bias model, the relation $r_* \approx r_o b^{-2/\gamma_*}$ gives

$$b = 1.11 \pm 0.22 \quad (28)$$

at one-sigma statistical significance level.

4.2. The relative velocity

We will now apply the second of the two proposed tests of biasing: the relative velocity test. We will compare the mean pairwise velocity, predicted by assuming that the APM galaxies trace the mass with the pairwise velocity, measured directly from a peculiar velocity – distance survey.

Figure 4 shows $v_{12}(r)$ curves, predicted by equation (5) (continuous lines) for three different values of Ω_m , from bottom to top $\Omega_m = 1.0, 0.3, 0.1$, respectively. To calculate $v_{12}(r)$, we have used $\xi(r)$, estimated from the APM survey under the assumptions $\xi_g = \xi$ and $R = 1$.

Before making the comparison, we must overcome the following problem. The survey has a significant depth, with the mean redshift of $z \simeq 0.15$ while the measured $v_{12}(r)$ corresponds to the present time ($z = 0$). To evolve $\xi(r, z)$ from $z \simeq 0.15$ to $z = 0$, we need to make some additional model assumptions. Gaztañaga (1995) has shown that for this redshift range, the uncertainties in the details of dynamical evolution of ξ are small. In particular, choosing an incorrect value for Ω_m can affect ξ at most at the several per cent level (for Ω_m ranging from 1 to 0). Adding this to other possible sources of errors, such as uncertainties regarding the redshift evolution of the galaxy number density and sampling and selection fluctuations, Gaztañaga (1995) estimates that the resulting relative uncertainty in the amplitude of ξ_g is $\lesssim 20\%$. According to his analysis, the present ($z = 0$) amplitude of the rms fluctuation of the APM galaxy counts, measured in spheres of radius of $8 h^{-1}\text{Mpc}$, is $1.1 \lesssim \sigma_8^{APM} \lesssim 0.9$.

To be conservative, for each value of Ω_m , we plot the predicted $v_{12}(r)$ curves for two values of σ_8 , differing by 20%. The resulting prediction for each value of Ω_m is therefore an area rather than a single $v_{12}(r)$ curve (see Figure 4). The lower boundary of each shaded area assumes $\sigma_8 = 1.1$ while the upper boundary was calculated by assuming $\sigma_8 = 0.9$. A direct measurement at $r = 10 h^{-1}$ from the Mark III galaxy peculiar velocity survey (Willick et al. 1997) gives (Juszkiewicz et al. 2000a)

$$v_{12} = -280 \pm 60 \text{ km/s} . \quad (29)$$

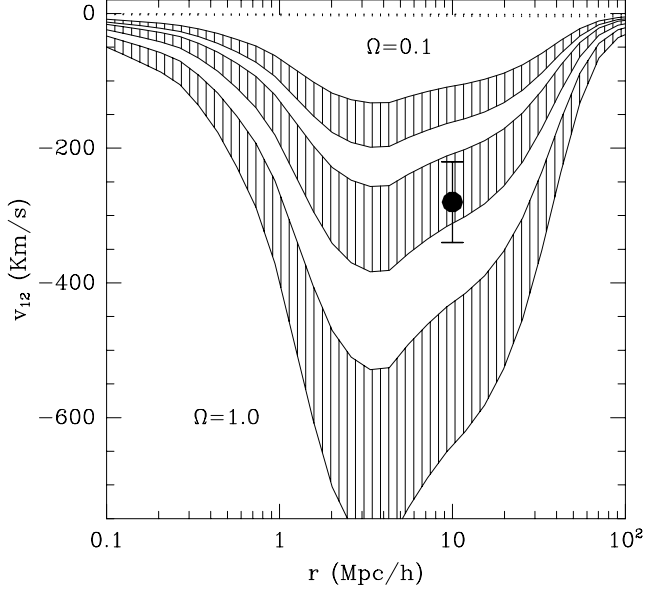


Figure 4. Predictions for the mean pairwise velocity v_{12} , based on the assumption that the APM galaxies trace the mass. The shaded regions correspond to 20% uncertainties in the strength of clustering. We consider three values of $\Omega_m = 1.0, 0.3, 0.1$, top to bottom (as labeled). The point with error bars corresponds to a direct measurement from the Mark III survey (Juszkiewicz et al. 2000a).

It is reassuring that this value, plotted in Figure 4, overlaps with the shaded area, corresponding to $\Omega_m = 0.3$, because it agrees with ranges for Ω_m and σ_8 obtained by Juszkiewicz et al. from the analysis of the Mark III survey alone. Their one-sigma constraints are $\Omega_m = 0.35^{+0.35}_{-0.25}$ and $\sigma_8 \geq 0.7$, and the analysis assumes that the correlation function for the mass is well approximated by a pure power law with $\gamma = 1.75$.

From the agreement between the predicted and observed value of the mean pairwise velocity, we conclude that the Mark III and APM data, taken together, are consistent with the hypothesis that the APM galaxies trace the mass, $b \approx R \approx 1$, while the density parameter is low, $\Omega_m \approx 0.3$.

4.3. How can biasing affect $v_{12}(r)$?

Apart from leading to predictions which are confirmed observationally, the “what you get is what you see” hypothesis has another important advantage: simplicity. Once $\xi(r)$ is estimated from observations, a family of $v_{12}(r, \Omega_m)$ curves can be calculated directly from equation (5) for any given range of values of the density parameter. This simplicity will immediately go away if we allow scale-dependent, stochastic and nonlinear biasing. A frank answer to the question posed in the

heading of this subsection would have to be “Only God (of biasing) knows”. Predicting $v_{12}(r)$ without resorting to massive numerical simulations would be simply impossible. We can get the idea of what is in store by considering only the leading order term in the perturbative expansion for $v_{12}(r)$ at large separations (Juszkiewicz et al. 2000b),

$$v_{12}(r) = -\frac{2}{3} H r f(\Omega_m) \bar{\xi}_{g\rho}(r) , \quad (30)$$

where $\bar{\xi}_{g\rho}(r) = (3/r^3) \int_0^r \xi_{g\rho}(x) x^2 dx$ is the galaxy-mass cross-correlation function,

$$\xi_{g\rho}(r) = \langle \delta(0) \delta_g(\vec{r}) \rangle , \quad (31)$$

averaged over a sphere of radius r . The function $\xi_{g\rho}$ describes the cross-correlations between the mass density and the density of galaxies in the velocity field survey, which in the case considered here would be the Mark III catalogue.

To make progress in our analysis, we will now generalize the definition of the stochasticity parameter introduced as a normalized cross-correlation of two random fields, δ and δ_g , measured at the same position in space. Instead, we will consider a cross-correlation of the same two fields measured at two different positions in space, separated by distance r . Our old equation (2) is replaced by

$$R(r) = \frac{\xi_{g\rho}(r)}{\sqrt{\xi(r) \xi_g(r)}} . \quad (32)$$

Let us make another simplifying assumption, that $b^2(r) \equiv \xi_g(r)/\xi(r)$, as well as R , are separation-independent. Equation (30) becomes

$$v_{12}(r) = -\frac{2}{3} f(\Omega_m) H r R b \bar{\xi}(r) . \quad (33)$$

The expected relative pairwise velocity can now be related to the APM data by substituting

$$\bar{\xi}(r) = \frac{3}{b_A^2 r^3} \int_0^r \xi_g(x) x^2 dx , \quad (34)$$

where $b_A^2 = \xi_g(r)/\xi(r)$ and ξ_g is the APM galaxy correlation function. In case of trouble in predicting the correct $v_{12}(r)$ curve, we now have three essentially free parameters which can be readjusted. This is only the tip of the iceberg, as we have ignored nonlinear dynamics as well as the scale-dependence of b and R .

For the linear bias model, the predictions are in clear conflict with the data unless b is close to unity. After setting $R = 1$, we get $v_{12}(r) \propto b$. Then, if the biasing factor for spiral galaxies is, as usually assumed $b \approx 1$, our predictions for $v_{12}(r)$ in the linear regime ($r \gtrsim 10 h^{-1} \text{Mpc}$) should be similar to the unbiased predictions already plotted in Figure (4). If the biasing factor for the ellipticals is significantly different, say, $b \approx 2$, the elliptical subsample of the Mark III data should give estimates of v_{12} which differ from the estimates from the spiral sample by the same factor of two. Meanwhile the estimates from the appropriate subsamples in the real data are indistinguishable (Juszkiewicz et al. 2000a). Hence, just as in case of the shape of the APM correlation function, considered above, the deterministic linear biasing model is inconsistent with observations.

We can summarize the last two subsections as follows. The prediction for $v_{12}(r)$, based on the assumption that the APM galaxies trace the mass passes our test as it agrees with the velocity, estimated from the Mark III data. The simplest prescription of biasing fails the test. More complicated prescriptions can probably be made to pass, which is not surprising, given the number of free parameters.

5. Summary and discussion

A quarter of a century ago, Gott and Rees predicted that gravity should leave its mark on the shape of the galaxy autocorrelation function: a “shoulder”, or steepening of the slope of the correlation function should appear near the separation where ξ passes through unity. At the time, biasing was unheard of, and Gott and Rees (1975) assumed $\xi = \xi_g$. Recently, in another context, JSD have studied the the $\xi = 1$ boundary in the evolution of the mass correlation function, using results from Virgo simulations. They found that the “shoulder” is actually an inflection point, occurring at a well defined separation r_* . In all four CDM-like models they studied, the nonlinear transition looked strikingly similar: the inflection occurred at almost the same separation as that of the nonlinear transition: $r_* \approx r_o$, where r_o corresponds to $\xi = 1$. Here we have tested the degree of universality of their results by widening the range of models considered. Our additional objective was to study the range of validity of an approximate solution of the pair conservation equation, proposed by JSD to study the nonlinear evolution of the relative velocity of particle pairs at a fixed separation, $v_{12}(r)$. We used N-body simulations, with APM-like initial conditions, with two different values of the density parameter: $\Omega_m = 1$ and 0.3. The APM-like initial power spectra differ significantly from all of the CDM-like spectra, considered earlier by JSD. Moreover the spectra of the latter kind appear as more realistic to us because they can reproduce observations without resorting to scale-dependent biasing. Our APM-like simulations are in excellent agreement with earlier results, confirming the validity of the JSD ansatz for $v_{12}(r)$ and the conjecture that the appearance of the shoulder in the correlation function near the $\xi = 1$ transition is a feature of gravitational dynamics rather than a peculiarity of a particular set of initial conditions.

Using these results, we proposed two tests of the hypothesis that galaxies trace mass. The first of the tests is based on an obvious idea, that if $\xi(r) = \xi_g(r)$, the galaxy correlation function near $\xi_g = 1$ should exhibit properties similar to those of the matter correlation function. We examined the behavior of the correlation function, derived from the APM catalogue and found exactly the same features we knew earlier from N-body simulations, in particular the agreement between the two characteristic scales, $r_* \approx r_o$. It is difficult to imagine how such an agreement could happen by a mere coincidence, which would have to be the case if ξ_g is unrelated to ξ . The agreement between the two characteristic scales can be used to constrain the linear biasing factor for the APM catalogue to be within 20% of unity. This constraint agrees with an earlier limit, obtained from measurements of the three-point correlation function from the APM survey (Gaztañaga 1994, Frieman & Gaztañaga 1999).

The second test confronts the v_{12} , predicted by assuming that the APM galaxies are unbiased tracers of mass with direct measurements of v_{12} . The results are again consistent with $b \approx 1$ and a low density parameter, $\Omega_m \approx 0.3$, in agreement with the limits obtained from the velocity data alone (Juszkiewicz et al. 2000a).

We are impressed how well the observations are reproduced by the simple calculations based on the assumption that galaxies follow the mass distribution, at least on large (weakly non-linear) scales. We are unable to constrain biasing models with a large number of free parameters, but their predictive power is questionable and one may ask: are such models falsifiable and therefore worth constraining?

Our results are by no means final, they are also less rigorous than one could wish because we are limited by the accuracy of the present observational data. New generation of catalogues promise a dramatic improvement on this front in the near future (for an excellent collection of reports on the state of the art in this field, see Colombi et al. 1998).

6. Acknowledgements

One of the co-authors (RJ) who was more lucky than the other and who attended this excellent Meeting would like to thank Jim Fry for making it happen. We also thank Carlton Baugh for providing us with his APM-like simulations as well as his estimate of $\xi_g(r)$, based on the APM survey. RJ thanks Ruth Durrer for important discussions regarding the inflection point in $\xi(r)$ and for her hospitality at the University of Geneva. This work was supported by a collaborative grant between the Polish Academy of Science and the Spanish Consejo Superior de Investigaciones Cientificas. We also acknowledge support by grants from the Polish Government (KBN grant No. 2.P03D.01719), the Swiss Tomalla Foundation, and from IEEC/CSIC and DGES(MEC) (Spain), project PB96-0925.

References

Binney, J., & Merrifield, M., 1998, Galactic Astronomy, Princeton University Press, Princeton

Baugh, C.M., 1996, MNRAS, 282, 1413

Baugh, C.M., & Gaztañaga, E., 1996, MNRAS, 280, 37

Bernardeau, F., 1994a, A&A, 291, 697

Bernardeau, F., 1994b, ApJ, 433, 1

Blanton, M., Cen, R., Ostriker, J.P., Strauss, M.A., 2000, ApJ, 531, 1

Colombi, S., Mellier, Y., & Raban, B., eds., 1998, Wide Field Surveys in Cosmology, Editions Frontieres, Paris.

Davis, M. & Peebles, P.J.E., 1977 ApJS, 34, 425

Davis, M. & Peebles, P.J.E., 1983, *ApJ*, 267, 465

Davis, M., Efstathiou, E., Frenk, C.S., White, C.D.M., 1985, *ApJ*, 292, 371

Dekel, A., & Lahav, O., 1999, *ApJ*, 520, 24

Feldman, H.A., Frieman, J.A., Fry, J.N. & Scoccimarro, R., 2000, preprint, astro-ph/0010205

Fischer, P., et al. (the SDSS Collaboration), 1999, preprint, astro-ph/9912119

Fisher, K.B., Davis, M., Strauss, M., Yahil A., Huchra, J. 1994, *MNRAS*, 267, 927

Frieman, J.A., Gaztañaga, E., 1999, *ApJ*, 521, L83

Fry, J. 1996, *ApJ*, 461, L65

Gaztañaga, E., 1994, *MNRAS*268, 913 (1994)

Gaztañaga, E., Frieman, J.A., 1994, *ApJ*, 437, L13

Gaztañaga, E. 1995, *ApJ*, 454, 561

Gott, J.R., & Rees, M.J., 1975, *A&A*, 45, 365

Guzzo, L., 1997, *New Astronomy*, 2, 517

Hamilton, A.J.S., 1998, in Hamilton D., ed., *The Evolving Universe*, Kluwer, Dordrecht, p. 185

Hamilton, A.J.S., Tegmark, M., & Padmanabhan, N., 2000, preprint (astro-ph/0004334)

Hamilton, A.J.S., Tegmark, M., 2000, preprint, astro-ph/0008392

Jenkins, A. et al. (The Virgo Consortium), 1998, *ApJ*, 499, 20

Juszkiewicz, R., Fisher, K., & Szapudi, I., 1998, *ApJ*, 504, L1

Juszkiewicz, R., Springel, V., & Durrer, R., 1999, *ApJ*, 518, L25 (JSD)

Juszkiewicz, R., Ferreira, P.G., Feldman, H.A., Jaffe, A.H., & Davis, M., 2000, *Science*, 287, 109

Juszkiewicz, R., Durrer, R., Ferreira, P., 2000, in “Energy densities in the Universe”, Proc. Recontres de Moriond, in press

Lokas, E., Juszkiewicz, R., Bouchet, F.R., & Hivon, E., 1996, *ApJ*, 467, 1

Peebles, P.J.E., 1980, *The Large-Scale Structure of the Universe*, Princeton University Press, Princeton (LSS)

Peebles, P.J.E., 1993), *Principles of Physical Cosmology*, Princeton University Press, Princeton

Peebles, P.J.E., 1999, in Clustering at High Redshift, eds. A. Mazure & O. Le Fevre (astro-ph/9910234)

Rees, M.J., 1999, preprint, astro-ph/9912373

Saunders, W., 2000, preprint, astro-ph/0001117

Seljak, U., 2000, preprint, astro-ph/0004086

Scoccimarro, R., & Frieman, J. 1996, ApJ, 473, 620

Scoccimarro, R., Sheth, R., Hui, L., & Jain, B., 2000, ApJ, in preparation

Somerville, R.S., et al., 2000, MNRAS, 320, 289

Strauss, M., Willick, J., 1995, Physics Reports, 26, 271

Van Waerbeke et al., 2001, preprint, astro-ph/0101511

Villumsen, J., & Davis, M., 1986, ApJ308, 499

Vittorio, N., Juszkiewicz, R., & Davis, M, 1986, Nature, 323, 132

Willick, J., et al., (1997), ApJS, 109, 333